BNL-108470-2015-JA

The Life Science X-ray Scattering Beamline at NSLS-II

Jonathan DiFabio[1], Shirish Chodankar[1], Sal Pjerov[1], Jean Jakoncic[1], Michael Lucas[1], Christina Krywka[1,2], Vito Graziano[1] and Lin Yang[1, a)]

[1] National Synchrotron Light Source II, Brookhaven National Laboratory, Upton, New York, USA
[2] On leave from Institut für Werkstoffforschung, Helmholtz-Zentrum Geesthacht, Hamburg, Germany

[a)] Corresponding author: lyang@bnl.gov

Abstract. We report the current development status of the High Brightness X-ray Scattering for Life Sciences (or Life Science X-ray Scattering, LiX) beamline at the NSLS-II facility of Brookhaven National Laboratory. This instrument will operate in the x-ray energy range of 2.1-18 keV, provide variable beam sizes from 1 micron to ~0.5 mm, and support user experiments in three scientific areas: (1) high-throughput solution scattering, in-line size exclusion chromatography and flow mixers-based time-resolved solution scattering of biological macro-molecules, (2) diffraction from single- and multi-layered lipid membranes, and (3) scattering-based scanning probe imaging of biological tissues. In order to satisfy the beam stability required for these experiments and to switch rapidly between different types of experiments, we have adopted a secondary source with refractive lenses for secondary focusing, a detector system consisting of three Pilatus detectors, and specialized experimental modules that can be quickly exchanged and each dedicated to a defined set of experiments. The construction of this beamline is on schedule for completion in September 2015. User experiments are expected to start in Spring 2016.

OPTICAL LAYOUT

In order to achieve the wide x-ray energy range and flexible focus size at the sample position, we have adopted an optical scheme of two-staged focusing (Fig.1a). In the first stage, a pair of KB mirrors focus the x-rays from the source to a secondary source aperture (SSA). A vertically deflecting, flat white beam mirror (WBM) is used to reduce the heat load on the monochromator crystal. The WBM also separates the white beam from Bremsstrahlung to simplify radiation shielding. The x-ray beam enters the experimental station horizontally, after being deflected twice in the vertical plane by the WBM and the vertical focusing mirror (VFM) of the KB pair. All mirrors have an incident angle of 3.5mrad, with a Pd-coated (cut-off energy ~18 keV) stripe and an uncoated Si stripe (cut-off energy ~9 keV). These reflecting optics are necessary to remove high-energy components in the undulator spectrum.

In the second focusing stage, beryllium compound refractive lenses (CRLs) are used either to re-focus the beam to the sample position, or to simply collimate the beam to achieve a large beam size with low divergence. CRLs are not suitable for low-energy experiments due to high x-ray absorption by the lens material. This is acceptable at the LiX beamline since the envisioned low-energy experiments require the grazing incidence geometry, using two short (10 cm) harmonic rejection mirrors (HRMs). The downstream HRM is bendable and provides vertical focusing.

To improve beam stability at the sample position, all hutches are normally closed to maintain temperature stability. The experimental hutch is equipped with a small sample access door to facilitate automated sample handling and avoid unnecessary hutch access. We therefore expected the beam instability to be mainly intensity fluctuation as the result of beam positional drifts at the secondary source, which can be attribute to pitch angle fluctuations of the reflecting mirrors, but predominantly to unstable monochromator crystals, since they are not as massive as the mirrors and are coupled to a vibration source (the liquid nitrogen cryo cooler). Ideally the planes in the two crystals must be parallel to each other. This is often not the case in reality, due to vibrations and temperature drifts in the positioning mechanics. While slight changes in the Bragg angle are inconsequential for the experiments at LiX, changes in the relative orientation between the two crystals would mis-steer the monochromatic beam astray.

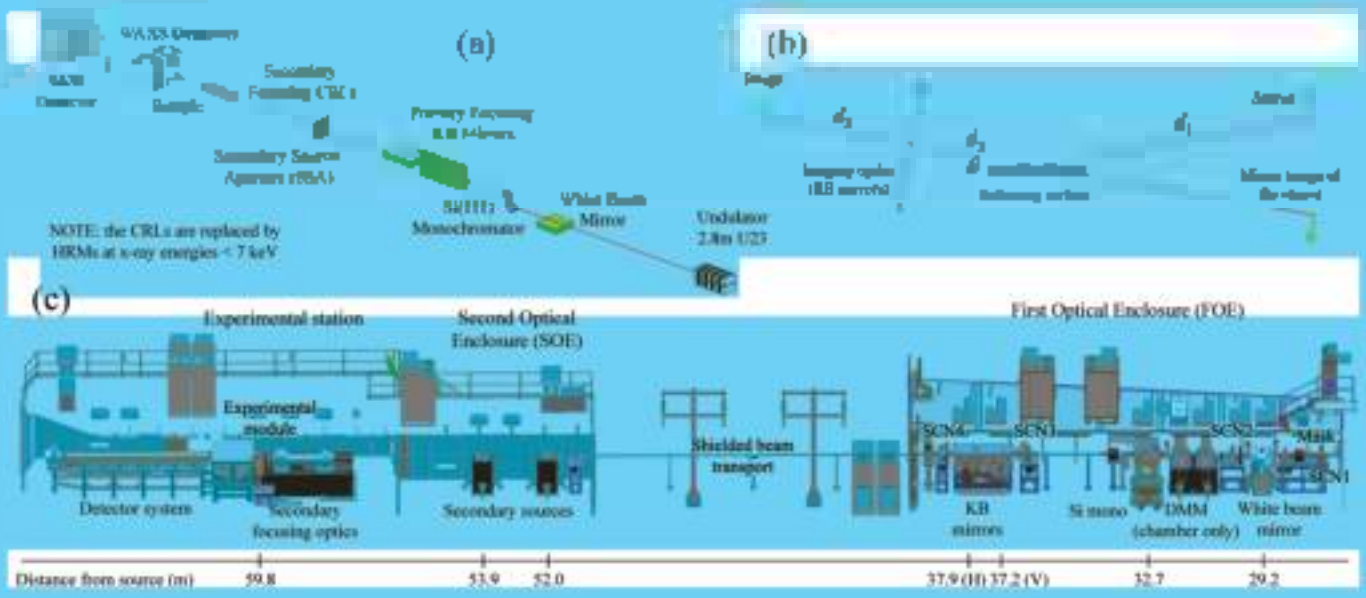

FIGURE 1. (a) Conceptual layout for the LiX beamline. See text for detailed descriptions. (b) Diagram for estimating the drift of the secondary source due to orientation fluctuations of reflective optics. (c) 3D engineering model for the entire LiX beamline.

The consequence of these orientational fluctuations can be quantitatively estimated as follows (Fig.1b). A change in the orientation ($d\theta$) of a reflecting surface would result in an apparent shift of the source position, which is imaged to the SSA by the KB mirrors. The resulted drift of the image, Δ, therefore is given by $d\theta$ and an equivalent level-arm length D: $\Delta \sim 2Dd\theta$, where $D = d_2 / (1 + d_2/d_1)$. We therefore located the monochromator and the WBM as further upstream as possible.

To accommodate experiments that require exceptional beam stability, we include in the monochromator a channel-cut crystal in additional to the fixed-exit pair (20mm offset) that is available throughout the energy range of 2.1-18 keV. The first crystal of the fixed-exit pair and the channel-cut crystal are fabricated from a single piece of silicon material so that they reflect the beam to the same direction. Crystal selection is realized by translating the entire monochromator chamber perpendicular to the beam direction. The use of the channel-cut crystal is limited to 8-16 keV since the beam offset depends on the Bragg angle, which can be compensated by simultaneously adjusting the incident angle on the WBM and the VFM.

The double multilayer monochromator (DMM) is currently only a chamber. The multilayers are planned as a future upgrade. Since the energy resolution is poor with the DMM, we envision using it only at a few discrete energies, by employing multilayers with multiple stripes of different periods positioned at a fixed incident angle.

DEVELOPMENT OF BEAMLINE COMPONENTS

The layout of the LiX beamline is shown in Fig.1c. In order to meet project schedule and realize specialized functionality, we develop smaller, one-of-a-kind components in-house, while let our contracts to build larger components based on our technical specifications. For diagnostics, the second crystal of the Si(111) monochromator and all deflecting mirrors are equipped with high-resolution encoders for monitoring vibrations. Several beam visualization screens are also installed along the beamline (SCN1-4 in Fig.1c).

Secondary Source

The SSA is a set of piezo-driven slits (PiezoSystem Jena PZS4). Its location is not adjustable and its aperture size can be precisely controlled. Polished tungsten rods are used as slit blades [1]. The SSA is integrated together with several other components for diagnostics and beam conditioning (Fig.2a).

A diamond quadrant beam position monitor (BPM, Sydor) is installed upstream of the SSA, mounted on two SmarAct stages so that its center position can be aligned to the SSA. The output of the diamond BPM will used to provide closed-loop feedback control to stabilize the observed beam position, by using the fine pitch motion either on the KB mirrors or on the second crystal of the monochromator.

The attenuator includes 5 types of absorbers (10 layers each, stacked in ~1.5 mm steps) for beam intensity adjustment throughout the full energy range of 2.1-18 keV (Fig.2b).

The shutter is based on a bistable solenoid (Gee Plus, BRS1020), so that it is powered only when switching. A scintillator is installed on the shutter blade. Whenever the shutter is closed, the beam shape can be monitored using a long working-distance microscope through the viewport and a drilled 90-degree mirror. Focusing of the microscope is adjusted by moving the picomotor-driven stage on which the shutter is mounted. The shutter drive electronics is based on a stepper motor driver as described by Scholten [2]. The resistor has been removed, since no holding current is required to maintain the shutter position. Using a high-speed camera, we were able to determine that it takes less than 5 ms for the shutter to switch between fully open and fully closed states (Fig.2c).

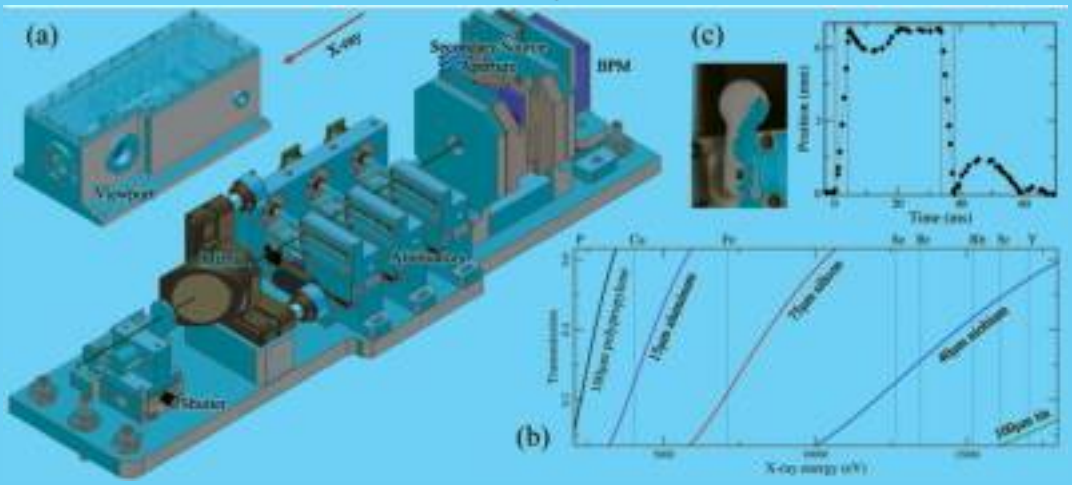

FIGURE 2. (a) The mechanical designs of the secondary source chamber and the internal components. (b) The expected x-ray transmission for a single absorber foil installed in the attenuator. The K absorption edges of relevant elements are indicated. (c) Test result of the shutter using a high-speed camera (3000 fps). The position of the shutter blade (as indicated by the "λ" in the still frame) is tracked as a function of time. Some rebounding is visible. The dotted lines indicate 4ms intervals.

A set of stepper motor-driven slits is installed at 1.9 m downstream of the SSA as an alternate SSA (see Fig.1c), so that the demagnification range for secondary focusing can be further adjusted.

CRL Transfocator for Secondary Focusing

All secondary focusing components are housed in a vacuum chamber (Fig.3a). Given the wide x-ray energy range, a large number of CRLs are needed to provide focal length in the range of 1-2 m. We have chosen lenses of radius of curvature R=0.1 mm, as a compromise between effective aperture and number of lenses required. 4 additional R=0.5 mm lenses are used to provide finer step when adjusting the focal length. 2D lenses (RX Optics) are used to keep the number of lenses manageable.

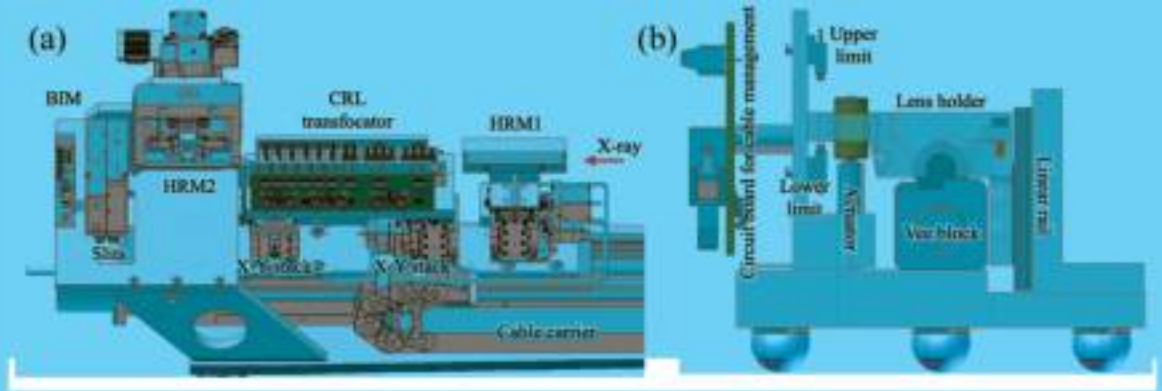

FIGURE 3. (a) Secondary focusing components inside the secondary focusing optics chamber. The BIM is a diamond BPM used as a beam intensity monitor. (b) Details of the CRL transfocator, viewed against the beam direction.

The lenses are organized in 9 lens holders in the transfocator. As shown in Fig.3b, each lens holder is driven by a linear actuator (MicroMo 0515A006B+06A) along a linear rail. The logic for enabling the motor driver (SC1801F) is implemented using a SN74LVC2G157 multiplexer IC, using the status of the limit switches and the drive direction as inputs. When driven to the "in beam" position, the CRL lenses are pushed by finger springs against a vee block to ensure that all lenses are aligned to the same axis.

The transfocator is mounted on two pairs of x-y stages at each of its ends for alignment. The entire structure is then mounted on a translation stage to provide variable working distance of the CRLs of ~0.7 – 2.1 m.

Experimental modules and on-axis microscope

The LiX beamline will need to be frequently reconfigured to accommodate different types of experiments. In order to minimize the effort to switch between experiments, we are designing experimental modules that are each dedicated to a class of experiments. These module share a common kinematic mounting interface with the granite base and can be removed and re-installed easily with high positional reproducibility. Figure 4 shows the experimental module for scattering-based scanning probe imaging and the on-axis microscope (QiOptics). Two other modules, one for solution scattering and another for grazing incidence scattering are also being developed.

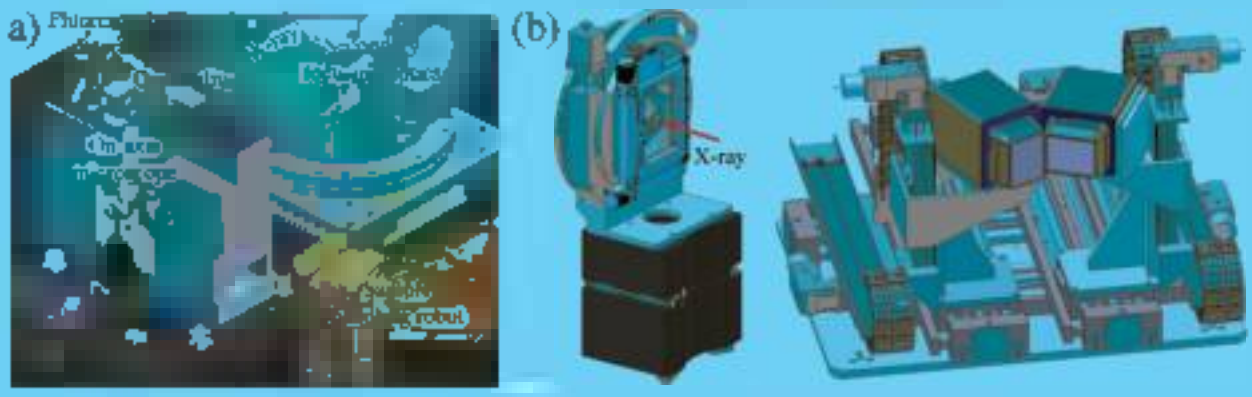

FIGURE 4. (a) Mounting interface for the experimental module and the nearby components. (b) The experimental module for scattering-based scanning probe imaging

FIGURE 5. Positioning mechanics for in-vacuum WAXS detectors.

Detector System

Three Pilatus detectors are used to collect scattering data simultaneously. The SAXS detector is a Pilatus3 1M. The flight path is based on bellows so that the camera length can be adjusted (2.3 – 5.9 m) while the flight path is under vacuum. Such a configuration has been implemented at other beamlines (e.g. [3]). The two Pilatus3 300K WAXS detectors are housed inside a large vacuum chamber, to give each detector an independently variable camera length of 0.2 – 0.8 m (Fig. 5). Combined, these detectors provide broad coverage in the reciprocal space.

ACKNOWLEDGMENTS

The LiX beamline is part of the Advanced Beamlines for Biological Investigations using X-rays (ABBIX) project funded by the National Institutes of Health. NSLS-II is supported by the U.S. Department of Energy, Office of Science, Office of Basic Energy Sciences, under Contract No. DE-SC0012704.

REFERENCES

1. D. Le Bolloc'h, F. Livet, F. Bley, T. Schülli, M. Veron, T.H. Metzger, J. Synch. Rad. **9(4)**, 258–65 (2002)
2. R.E. Scholten, Rev. Sci. Instr. **78(2)**, 026101 (2007)
3. A. Buffet, A. Rothkirch, R. Döhrmann, V. Körstgens, M.M. Abul Kashem, J. Perlich, et al. J. Synch. Rad. **19(4)**, 647-653 (2012)